Characterization of uniaxial fatigue behavior of precipitate strengthened Cu-Ni-Si alloy (SICLANIC®)

B. Saadouki, M. Elghorba

Laboratory of Control and Mechanical Characterization of Materials and Structures, National Higher School of Electricity and Mechanics. Casablanca, Morocco.
bouchra.saadouki@gmail.com

PH. Pelca

Lebronze alloys – Bornel, 11, rue Ménillet - 60540 Bornel – France

T. Sapanathan, M. Rachik

Sorbonne Universités, Université de Technologie de Compiègne, Laboratoire Roberval, CNRS UMR - 7337, Centre de Recherche Royallieu, CS 60319, 60203 Compiègne Cedex, France

ABSTRACT. Fatigue tests were conducted on cylindrical bars specimens to understand the fatigue behavior of SICLANIC®. Although it displays good resistance in monotonic tension, this material weakens and shows a softening in repeated solicitation. This has been verified through a SEM observation, the Cu-Ni-Si alloy presents transgranular failure by cleavage. The Manson-Coffin diagram exhibited the plastic deformation accommodation. The plastic deformation becomes periodic and decreases progressively as the cycle number increases. The approximations of Manson Coffin give fatigue parameters values which are in good agreement with the experience.

KEYWORDS. Fatigue; Copper alloy; S-N curve; Softening; Fracture.

INTRODUCTION

A t present, increasing demand for copper and copper alloys leads to the all-time high price of copper. Copper is widely used in electrical, electronic and thermal applications. Particularly, in an application where the high conductivity of copper is required, one should choose a copper alloy with higher percentage of copper, while there is a compromise required with the mechanical properties of the alloy. Hence, recent developments of copper alloys mainly focus on this issue and adapt to various strengthening mechanisms, such as precipitation hardening. Precipitates hardened copper alloys contain additive elements in small quantities that improves the mechanical characteristics by forming precipitates, without greatly altering their electrical conductivity [1]. The mechanical strength of these alloys is improved by precipitation of the secondary phase particles during the quenching and tempering heat treatment processes [2-4]. Thus,

the precipitation hardened copper alloys offer cost saving and they are suitable for many industrial applications under various mechanical loading conditions.

Cu-Ni-Si alloys strengthened by precipitation hardening are used in very wide range of electrical and electromagnetic applications. However, the cyclic circulation of alternating current induces fatigue failure during the high frequency electromagnetic applications [5]. Fatigue behavior of Cu-Ni-Si alloys has been investigated in few articles [6- 9]. In [6], authors investigated the microstructure of the material at different heat treatment states and its influence on the low cycle fatigue (LCF) and high cycle fatigue (HCF). They have noticed a softening effect of the copper alloy under LCF [6].

Goto *et al.* [8] studied the role of the Ni_2Si curing compound in fatigue crack initiation and propagation mechanism and identified a localized fatigue behavior. Zhao *et al.* [9] agree that the curing compound in Cu-Ni-Si is coherent with the matrix. Consequently, the main mechanism of crossing the secondary phase (Ni_2Si) by a sliding dislocation is shearing.

Besides, the alloys studied are of a different chemical composition than that of proposed in this work. This work is proposed to determine the fatigue characteristics for a Cu-Ni-Si alloy known by its trade name of SICLANIC®. The SICLANIC® is also strengthened by the precipitation of the Ni_2Si phase [10]. This alloy was mainly studied from a microstructure based investigation [11, 12]; while there exist few other studies with the focus on the mechanical aspects [13, 14]. However, fatigue properties of this alloy has never been reported before in the literature.

Fatigue test results are often represented by probabilistic Wöhler curve using statistical method and this curve has been developed due to the dispersions of tests results. In recent years, Castillo and Fernández-Canteli worked on the statistical analysis of the S-N and E-N fatigue curves [15], and they extended the probabilistic model to the strain damage evaluation to estimate fatigue life prediction in many applications [16, 17]. In this study, the probabilistic model of ASTM E 739[18] is applied to estimate Wöhler curves.

MATERIAL AND EXPERIMENTAL PROCEDURES

SICLANIC® alloy used in this study has the chemical composition with 96.9 % of copper, 2.5 % nickel and 0.6 % silicon in weight percent. The material has been received in bars of 14 mm × 14 mm× 60 mm dimension. To optimize high cycle fatigue tests, we chose classical specimen shape with circular section according to the ASTM E466-07 standard (Fig. 1) at MOROCCO CETIM.

The fatigue tests were carried out on an MTS biaxial hydraulic machine model 17 with imposed stress at a temperature of 20 °C. During the tests, the temperature was controlled using a thermocouple (Fig. 2). Solicitations were loaded in uniaxial cyclical mode, with a sinusoidal waveform, according to repeated tensile loads.
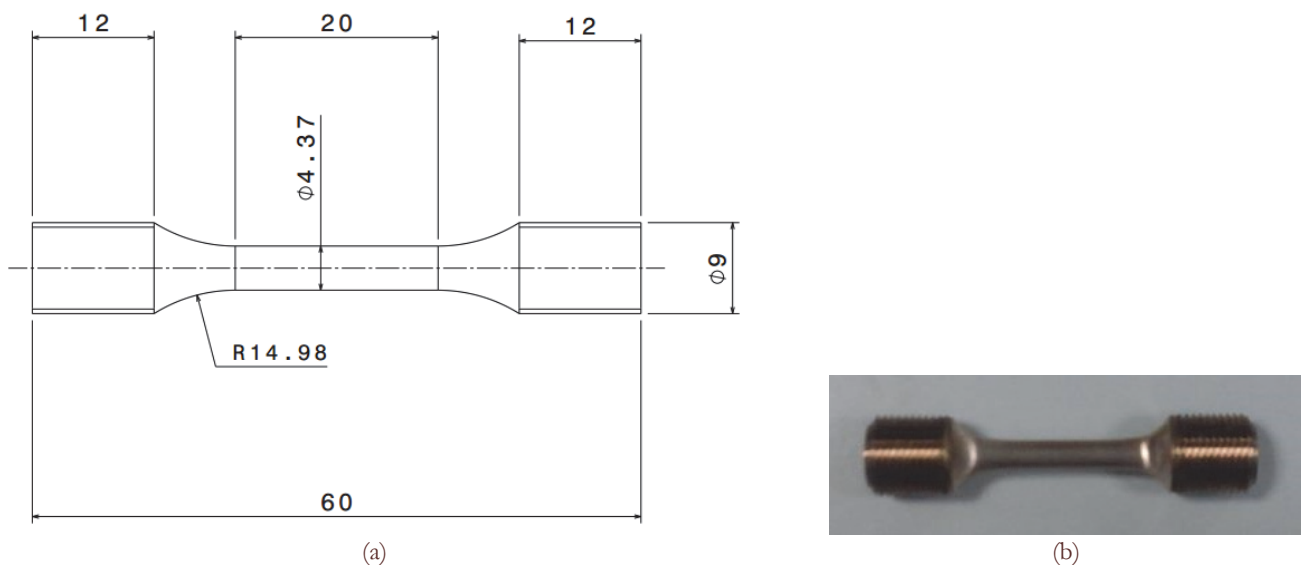

(a) (b)

Figure 1: Fatigue specimen (a) schematic illustration showing the specimen geometry and (b) image of the actual fatigue specimen.
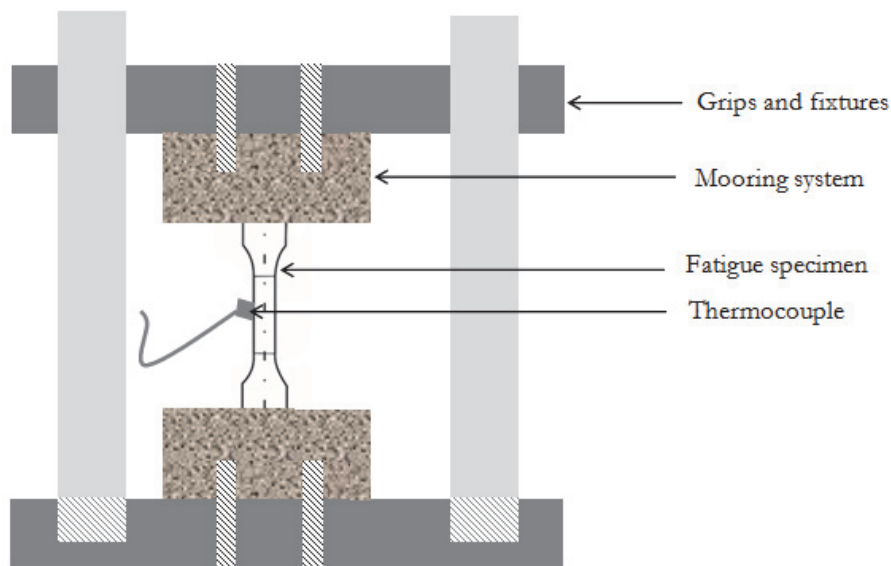
Figure 2: Schematic illustration of the experimental apparatus.

$$\sigma_a = \frac{\sigma_{max} - \sigma_{min}}{2} \qquad (1)$$

$$\sigma_m = \frac{\sigma_{max} + \sigma_{min}}{2} \qquad (2)$$

And the ratio of extreme stresses (maximum and minimum), also called load ratio and defined by:

$$R = \frac{\sigma_{min}}{\sigma_{max}} \qquad (3)$$

where, σ_{min} and σ_{max} are respectively the minimum and maximum stresses to which the specimen is subjected. The tests are conducted with zero-based loading at stress ratio $R = 0$ (Fig. 3), this implies the following equations:

$$\sigma_m = \sigma_a = \frac{\sigma_{max}}{2} \qquad (4)$$

$$\Delta\sigma = \sigma_{max} \qquad (5)$$

RESULTS AND ANALYSIS

Fatigue tests of studied material should be preceded by mechanical analysis of his answers to simple solicitation through tensile tests. Starting fatigue tests requires the definition of the first value of the maximum imposed stress.

Monotonic tensile behavior
Tensile tests have been carried out to characterize the monotonic properties of the material. Tests were conducted until the failure on a Zwick Roell machine under displacement mode. An additional test where an extensometer was used to the gauge length was performed to measure accurately the Young modulus. Monotonic tensile properties values are summarized in Tab. 1.
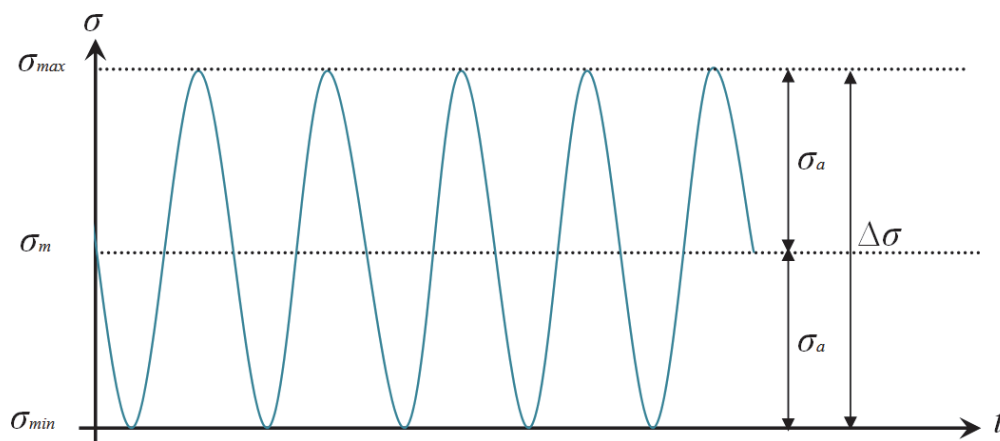
Figure 3: Tensile repeated solicitation on fatigue test.

E (GPa)	YS₀.₂% (MPa)	UTS (MPa)	A (%)	n	K (MPa)
121	498	615	11.62	0.034	591

Table 1: Monotonic tensile characteristics of the SICLANIC®.

Furthermore, the remarkable tensile strength of 615 MPa enhanced by the presence of silicon, the SICLANIC® has an elongation at fracture of higher than 10%. This ductility is mainly due to the high temperature of the solution treatment-quench phase during the hardening treatment.

The progressive passage, in the stress-strain curve, from linear elasticity to plastic deformation requires the definition of the conventional yield strength $YS_{0.2\%}$ which is of the order of 498 MPa. From this stress value, we realize a low permanent elongation which can be measured accurately. Mechanical behavior ceases to be elastic to become plastic.

S-N curve

SICLANIC® fatigue results show significant dispersion. This dispersion is now considered as one of physical fatigue aspects [19]. Indeed, for the same material, and the same load level, the lifetime may be different.

Iso-probabilistic S-N curve

As it is, the fatigue curve gives a tendency on the material behavior, but it is of limited use: we know that for a given stress level, half the specimens break for cycle number less than $N(\sigma)$, the other half breaks for cycle number more than $N(\sigma)$. For given stress level, the ratio between maximum and minimum value of failure cycle can exceed 10.

In a probabilistic concept, Wöhler curve represents the border separating the area where failure is less likely (left of the curve) to the area where failure is most likely (right part of the curve).

The fatigue life is generally described by the statistical longevity curve called iso-probabilistic Wöhler curve or median curve (N50, that to say 50% of survival specimens) [20]. For the SICLANIC®, fatigue curve median is illustrated in Fig. 4.

Probabilistic S-N curve

The confidence interval method using the probability of Student's law is also frequent to characterize fatigue behavior. It does not estimate directly the number of cycle to failure, but the estimations have percentage chance to containing the N_f. Thus, it is interesting to work in confidence interval of 80% that will give proper framing 80 times out of 100 on average, which meaning, if we could repeat the same tests a large number of times, affirming each time than N_f is in this interval, we would be wrong 20 times out of 100 on average. Fig. 5 shows SICLANIC® probabilistic Wöhler curve corresponding at 80% of survival, such a curve is sometimes called "curve design".
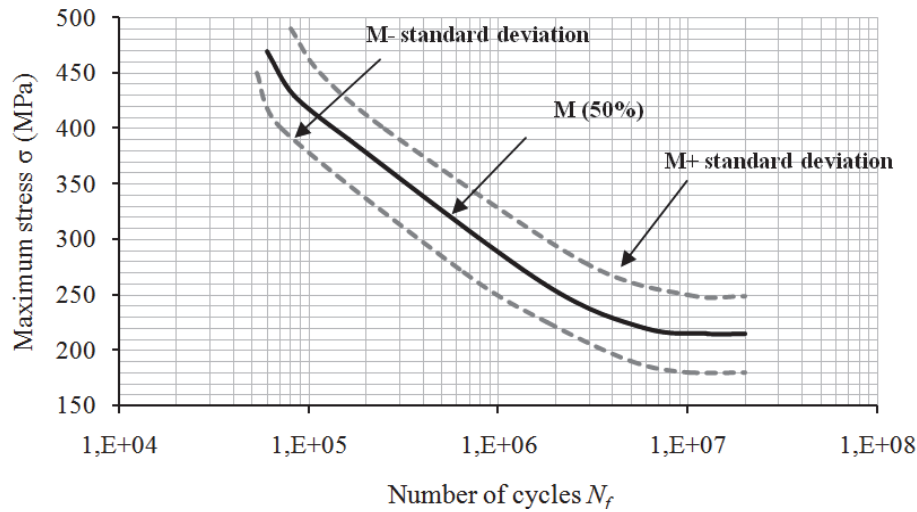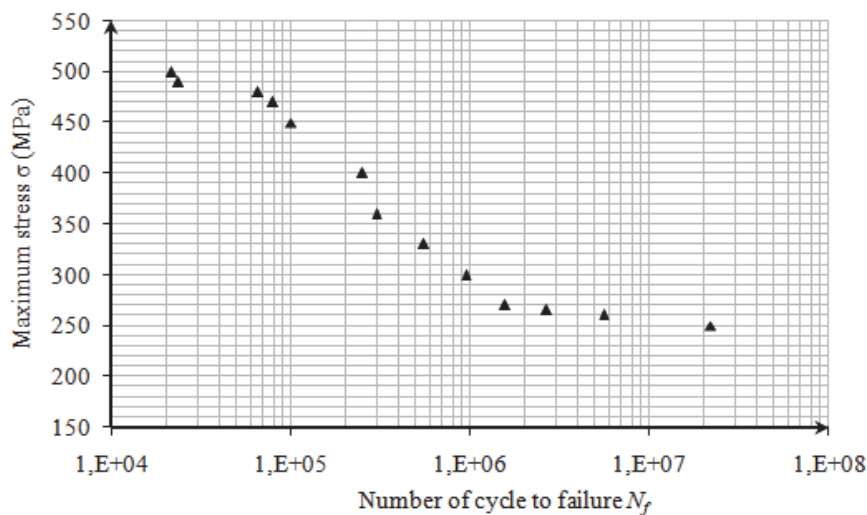
Figure 4: Median Wöhler curve for SICLANIC®

Figure 5: SICLANIC® probabilistic Wöhler curve at 80% chance of survival

The two probability methods appear in good agreement; they give very close values of the endurance limit. The estimated value of SICLANIC® endurance limit is 250 MPa.

Fractography

Fatigue fracture surfaces of SICLANIC® are often irregular; the majority of them are planar and perpendicular to the stress axis. Fig. 6 shows the fracture surface specimen which failed in 5×10^5 cycles. A fatigue fracture surface consists of three regions associated with crack initiation, crack growth, and final overload.

The darker region (ZA zone) presents the initial fatigue and slow crack growth in one or a few load cycles (Fig. 7). Surface crack initiation is located in the same area for all specimen tests. For certain specimens, we notice the existence of two crack initiation sites, one next to the other.

Beach marks (macroscale) and striations (microscale) in surface indicate fatigue loading. Failure by cleavage proves that we are at the brittle failure case, which is common for long-life fatigue. Cleavage occurs by direct separation along crystallographic planes, and the failure is transgranular.
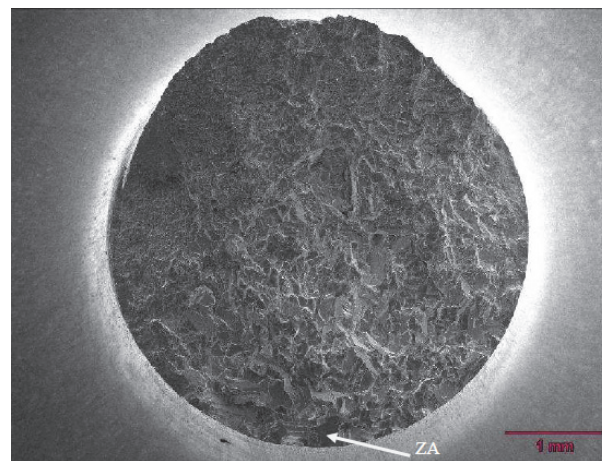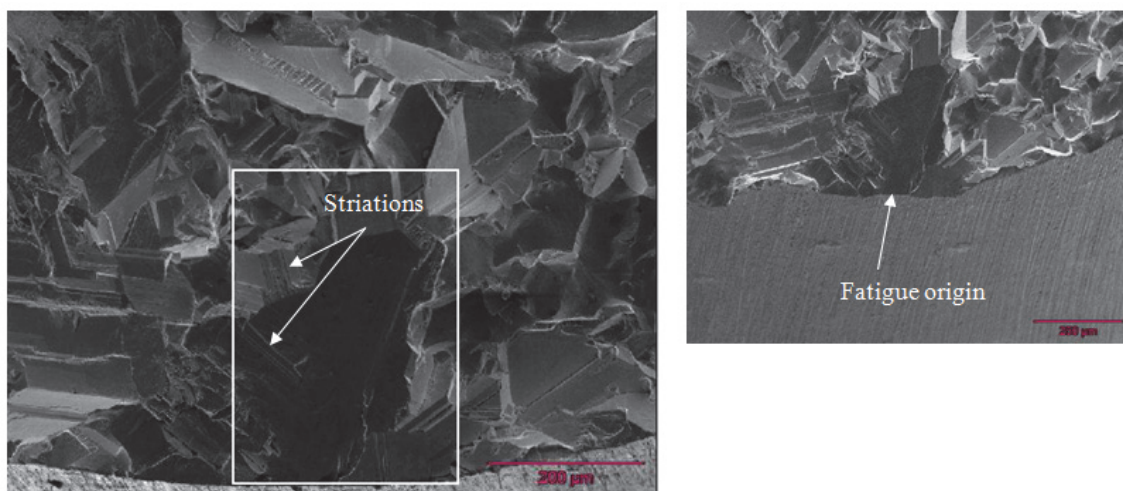
Figure 6: Fracture surface of the specimen.

Figure 7: Fatigue failure initiation site on cleavage planes of global dimension highlighted in the white box have approximately 426 μm ×284 μm.

Low cycle fatigue behavior

Cyclical behavior law

The comparison between the cyclic behavior curve and monotonic behavior curve reveals a softening during the cyclic loading (Fig. 8). The conventional yield strength falling of 19% in the cyclic tensile. Hardening or softening phenomena depend on the materials and their heat treatments. So, the evolution of fatigue mechanical characteristics depends on the initial state of the solid solution [21]. Softening is generally observed for steels whose structures are naturally work hardened by quenching and tempering, this softening corresponds to a decrease of the yield strength which can reach 30%. Similarly, SICLANIC® structural hardening by heat treatment of quenching and tempering leads to a stable phase represents a cyclical softening. The softening of SICLANIC® is similar to the others Cu-Ni-Si alloys behavior in low cycle fatigue, such behavior is usually attributed to the formation of intense bands of slip in which the precipitation hardening effect has been reduced [2].

In structural analysis, design of parts is based on yield strength *YS*, however, for SICLANIC®, which has a cyclic softening in fatigue solicitation ($YS'_{0.2} < YS_{0.2}$), even a cycle level of $\sigma_a < YS_{0.2}$, could result a deformation higher than ε_{max} and placing the piece out of service.

The following equation describes the cyclic behavior:

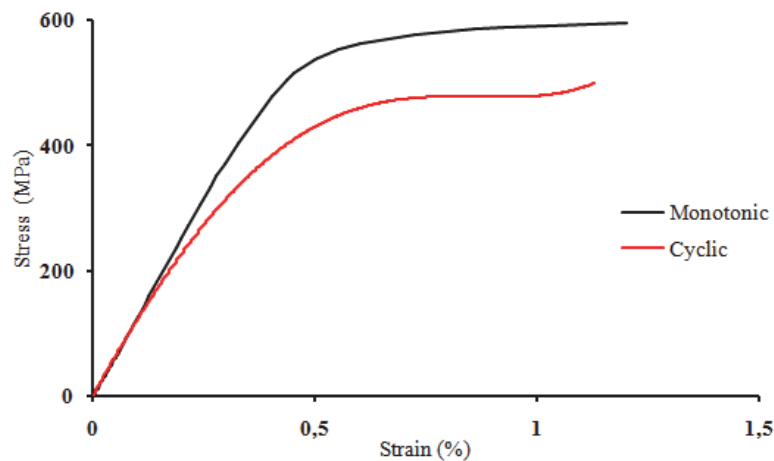$$\Delta\sigma = K'\Delta\varepsilon^{n'} \tag{6}$$

Figure 8: Comparison between monotonic and cyclic tensile curves for SICLANIC®.

It is the law of cyclic consolidation or cyclic hardening law, where K' and n' are respectively the coefficient and the exponent of cyclic hardening.

In Tab. 2, the monotonic and cyclic mechanical characteristics of SICLANIC® are compared. The extent of variation of the hardening coefficient is due to the cyclic deformation. It goes from a relatively low value (0.034) to a higher value of 0.136.

Monotonous	$n = 0.034$	$K = 591$ MPa	$YS_{0,2\%} = 498$ MPa
Cyclic	$n' = 0.136$	$K' = 490$ MPa	$YS'_{0,2\%} = 350$ MPa

Table 2: monotonic and cyclic mechanical characteristics of SICLANIC®

Prediction of softening or hardening phenomena

According to Smith, Hirschberg and Manson [22], softening occurs when $UTS / YS_{0.2} < 1.2$, while hardening appears for $UTS / YS_{0.2} > 1.4$. In the case where the ratio is between 1.2 and 1.4, one or the other of the softening and hardening phenomena can be observed.

As a result of the examination of various materials, Morrow [23] finds that if the value of n is higher than 0.1, hardening or stability occurs; however, if n is less than 0.1 the softening happens during the material is cycling.

In Tab. 3, we have compiled the predictions of SICLANIC® cyclical behavior, the predictions are in agreement with experience, however, the criteria used consider the characteristics determined outside the deformation domain (<2%) such as UTS and n.

A new definition of the hardening criteria is introduced by Lieurade [24], taking the ratio $\sigma_1 / YS_{0.2}$, of which parameters correspond to the experience, since they are located in plastic deformation field. It has been shown in the case of steels that if $\sigma_1 / YS_{0.2}$ is less than 1.3 there is softening, while if $\sigma_1 / YS_{0.2}$ is higher than 1.5 there is hardening.

Smith, Hirschberg, Manson		Morrow		Experience	$\sigma_1 / YS_{0,2}$		$\Delta\sigma_1 / \sigma_1$ (%)
$UTS / YS_{0.2}$	Prediction	n	Prediction	Observation	$\sigma_1 / YS_{0.2}$	Prediction	
1.23	uncertainty	0.034	softening	softening	1.18	softening	17.8

Table 3: Analysis of SICLANIC® hardening criteria.

The ratio $\Delta\sigma_1 / \sigma_1$ defines the hardening rate.

Plastic strain energy

Many researchers have used the cyclic plastic strain energy as damage criterion in low cycle fatigue. The dissipation of the mechanical energy is initially caused by the cyclic plastic strain connected, at microscopic level, to the dislocation movement and then, by the stress which relates to these dislocations resistance of displacement.

If we consider ΔW the mechanical energy per cycle as design parameter, the law of simple damage consists in supposing that there will be a failure when the total energy W_f has reached a critical value.

Halford [25] proposed a relation for measurement of the area under the hysteresis loop (Fig. 9), provided that the stress and the plastic strain are measured from the tip of the loop.
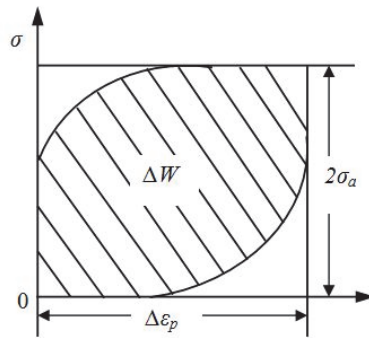

Figure 9: Area under hysteresis loop [26].

In the majority of cases, the difference between the energy measured directly from the hysteresis curve by a planimeter and that calculated by Eq. (7) is less than 10%.

$$\Delta W = \Delta \sigma \cdot \Delta \varepsilon_p \cdot \left(\frac{1-n'}{1+n'} \right) \tag{7}$$

where n' is the cyclic hardening coefficient.

The total energy to failure W_f is defined by the Eq. (8):

$$W_f = N_f \times \Delta W \tag{8}$$

Fig. 10 shows a significant decrease in mechanical energy ΔW per cycle when the number of cycles increases. Practically this energy does not vary during a test since $\Delta \varepsilon$ and $\Delta \sigma$ evolve inversely. The experimental points are placed around a curve corresponding to the following relation:

$$\Delta W = 0.364 N_R^{-0.44} \tag{9}$$

On the other hand, there is an increase in the total energy to failure W_f when the number of cycles increases (Fig. 11).
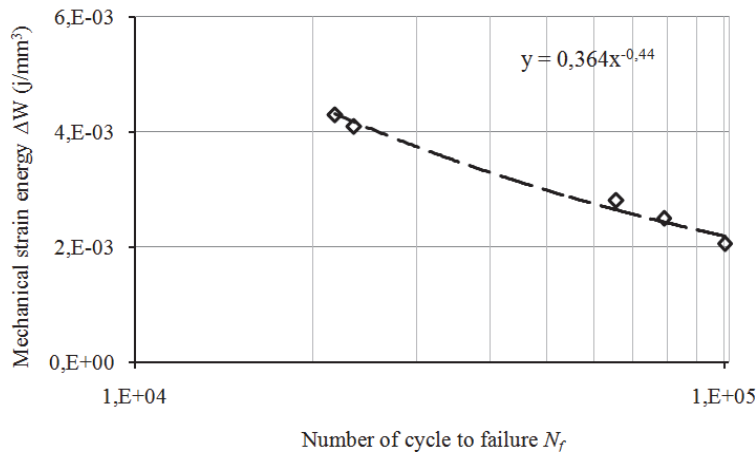

Figure 10: Evolution of mechanical energy per cycle in terms of fatigue lifetime.
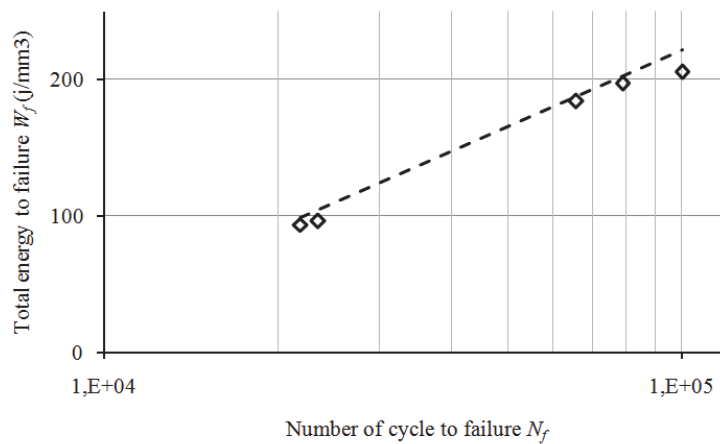
Figure 11: Variation of the total energy to failure as function of fatigue lifetime.

Fatigue resistance

Basquin and Manson-Coffin defined experimentally laws characterizing low cycle fatigue life, between strain variations $\Delta\varepsilon$ and the fatigue life.

- Manson-Coffin relation:

$$\frac{\Delta\varepsilon}{2} = \varepsilon'\left(2N_R\right)^c \tag{10}$$

- Basquin relation:

$$\frac{\Delta\varepsilon_{el}}{2} = \frac{\sigma_f'}{E}\left(2N_R\right)^b \tag{11}$$

SICLANIC® cyclic tests were conducted at imposed stress, achievement of fatigue resistance curves $\varepsilon - N$ cannot be direct. We used prediction formulas. These formulas have been proposed in principle to limit the number of tests and to avoid even realize one fatigue test.

The resistance relations fatigues are predicted by two methods, whose coordinates come from monotonic characteristic of the alloy.

    a) Four correlation point method

This method developed by Manson and Halford [25], allows the plot of elastic and plastic lines by knowing some monotonic characteristics.

    b) Universal slopes method

A second estimation method for resistance curves is proposed [27]. Manson, after many tests on various materials, made the followings hypotheses: elastic and plastic lines have respectively mean slopes of -0.12 and -0.6.

The points corresponding to the total strain variations $\Delta\varepsilon_t$ are placed on an asymptotic curve to the elastic and plastic lines. For low cycle fatigue, plastic strain predominates. The curve representing the plastic strain variation is placed above that of elastic strain up to a certain number of cycles (Fig. 12). SICLANIC® damage behavior, at low number of cycles, is accommodated by plastic cyclic strain. In approximating of the yield stress, plasticizing will be located at certain points of the alloy structure.

The plastic strain curve presents an important slope; this reflects the high gradient of this parameter. This gradient is a sign of cracks priming. Approximation methods appear in agreement at the strain values. However, this agreement is not verified for the number of cycles in transition point P_{Tr}. The universal slopes method seems most pertinent.

The elastic line expressing SICLANIC® resistance is located in the same order as the monotonic characteristics *UTS* and $YS_{0.2\%}$. For the plastic line, the capacity of plastic cyclical strain is dependent on the ductility; it operates to the same effect as this last. In terms of total strain, the SICLANIC® resistance is closely linked to materiel ductility at low cycle

(predominance of $\Delta\varepsilon_p$-N relation), and the yield strength and ultimate tensile strength at high cycle (predominance of $\Delta\varepsilon_{el}$-N).

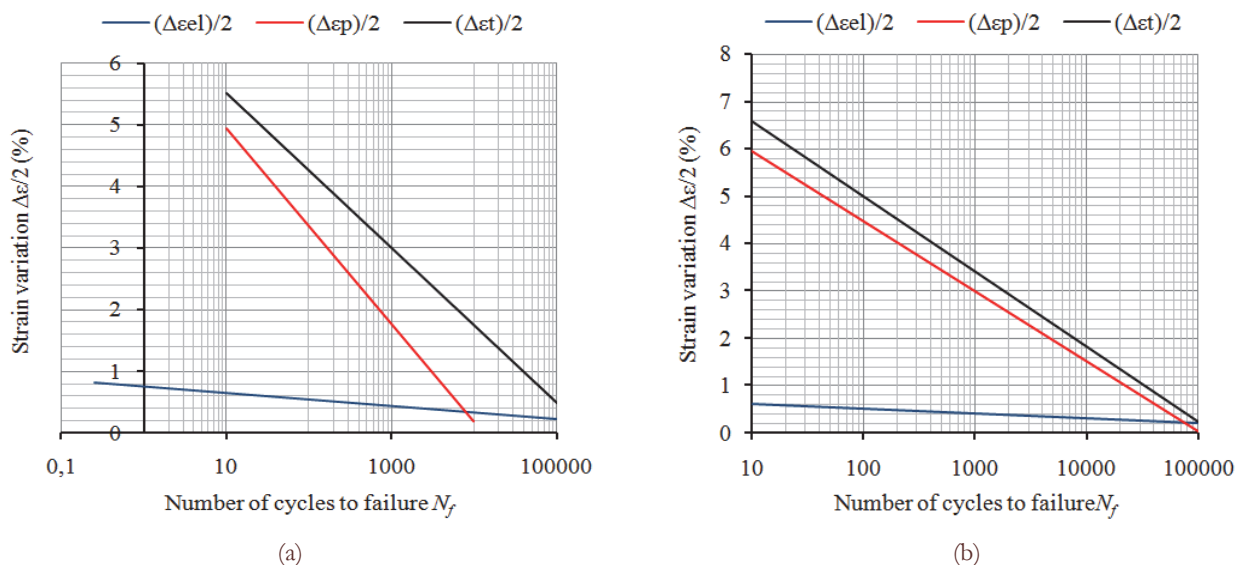Figure 12: Resistance fatigue curves for SICLANIC® predicted using (a) four correlation point method and (b) a universal slopes method.

	ε_f	σ_f (MPa)	ε_f'	σ_f' (MPa)	b	c
Manson's four points	0.29	793.35	0.19	931.71	-0.09	-0.46
Manson's universal slopes	0.29	793.35	0.36	1168.5	-0.12	-0.6

Table 4: Low cycle fatigue characteristics for the SICLANIC®.

Moreover, many researchers have linked coefficients *b* and *c* to the cyclic hardening coefficient *n'*, Tab. 5 shows some formulas results. Morrow has proposed the following relation:

$$b = -\frac{n'}{1+5n'} \tag{12}$$

$$c = -\frac{1}{1+5n'} \tag{13}$$

Tomkins [28] proposes on his side:

$$b = -\frac{n'}{1+2n'} \tag{14}$$

$$c = -\frac{1}{1+2n'} \tag{15}$$

	b			c	
Morrow	Tomkins	Manson-Coffin	Morrow	Tomkins	Manson-Coffin
-0.09	-0.1	-0.12	-0.59	-0.79	-0.6

Table 5: Comparison of the SICLANIC® fatigue exponent by different formulas.

The values of *b* and *c* suggested by Manson-Coffin are close to those obtained by using Morrow and Tomkins relations. These numerical expressions based on the coefficient of hardening n' calculated experimentally are in good agreement with the Manson-Coffin approximations.

CONCLUSIONS

Mechanical characterization of SICLANIC® proves that it is an alloy with high tensile characteristics. However, in cyclical loading, material shows moderate fatigue resistance. Results for fatigue analysis summarized as follows:
1. The mechanical properties (yield strength, hardening coefficient) of the SICLANIC® are considerably modified by the application of high stress cycles, even in small numbers. The SICLANIC® is softened under the fatigue loading. Hardening coefficient calculation with analytical models also predicts SICLANIC® softening phenomena.
2. If certain cycles reach stress levels close to or even more than $YS_{0.2}$, we can meet a softening behavior, so a lowering of The $YS_{0.2}$ up to $YS'_{0.2}$. High stress levels can cause harmful and permanent deformations to the proper functioning of the part.
3. The fractography analysis of the SICLANIC® specimens exhibits a transgranular failure during a cyclic solicitation. Fractures arise at the grain boundaries, and flat surfaces in the crystalline material confirms the cleavage failure.

ACKNOWLEDGEMENTS

REFERENCES

[1] Hornbogen, E., Hundred years of precipitation hardening. Journal of light Metal, 11 (2010) 127–132.
[2] Lockyer, S.A., Noble, F.W., Fatigue of precipitate strengthened Cu-Ni-Si alloy, Materials Science and Technology, 15 (1999) 1147-1153. DOI: 10.1179/026708399101505194
[3] Batawi, E., Morris, D.G., Morris, M.A., Effect of small alloying additions on behavior of rapidly solidified Cu-Cr alloys, Materials Science and Technology, 6 (1990) 892-899. DOI: 10.1179/mst.1990.6.9.892
[4] Lee, K.L., Whitehouse, A.F., Withers, P.J., Daymond, M.R., Neutron diffraction study of the deformation behavior of deformation processed copper–chromium composites, Materials Science and Engineering, A384 (2003) 208-216. DOI: 10.1016/S0921-5093 (02)00688-3
[5] Chen, X.P., Sun, H.F., Wang, L.X., Liu, Q., on recrystallization texture and magnetic property of Cu-Ni alloys, Materials Characterization, 121(2016) 149-156. DOI: 10.1016/j.matchar.2016.10.006
[6] Delbove, M., Vogt, J.B., Bouquerel, J., Soreau, T., Primaux, F., Low cycle fatigue behavior of a precipitation hardened Cu-Ni-Si alloy, International Journal of Fatigue, 92 (2016) 313–320. DOI: 10.1016/j.ijfatigue.2016.07.019.
[7] Sun, Z., Laitemb, C., Vincen, A., Dynamic embrittlement at intermediate temperature in a Cu–Ni–Si alloy, Materials Science and Engineering, A477 (2008) 145–152. DOI: 10.1016/j.msea.2007.05.013.

[8] Goto, M., Han, S.Z., Lim, S.H., Kitamura, J., Fujimura, T., Ahn, J.H., Yamamoto, T., Kim, S., Lee, J., Role of microstructure on initiation and propagation of fatigue cracks in precipitate strengthened Cu–Ni–Si alloy, International Journal of Fatigue, 87(2016) 15–21. DOI: 10.2472/jsms.63.401

[9] Zhao, D.M., Dong, Q.M., Liu, P., Kang, B.X., Huang, J.L., JIN, Z.H., Structure and strength of the age hardened Cu-Ni-Si alloy, Materials Chemistry and Physics, 79(2003) 81-86. DOI: 10.1016/S0254-0584(02)00451-0.

[10] Fujiwara, H., Sato, T., Kamio, A., Effect of alloy composition on precipitation behavior in Cu-Ni-Si alloys, Journal of the Japan Institute of Metals, 62 (1998) 301-309. DOI: 10.2472/jsms.63.401.

[11] Khereddine, A., Hadj Larbi, F., and al, Microstructures and textures of a Cu–Ni–Si alloy processed by high-pressure torsion, Journal of Alloys and Compounds, 574(2013) 361-367. DOI: 10.1016/j.jallcom.2013.05.051.

[12] Hadj Larbi, F., Azzeddine, H., Baudin, T., et al, Microstructure and texture evolution in a Cu–Ni–Si alloy processed by equal-channel angular pressing, Journal of Alloys and Compounds, 638(2015) 88-94.
DOI: 10.1016/j.jallcom.2015.03.062.

[13] Ageladarakis, P., O'Dowd, N., Webster, G., Tensile and fracture toughness test of CuNiSi at room and cryogenic temperatures, Commission of the European Communities, Abingdon (United Kingdom). JET Joint Undertaking, Available from British Library Document Supply Centre- DSC: 4672.2625(99/01).

[14] Reed, R., Fickett, F.R., Summers, L.T., Stieg, M., Advances in Cryogenic Engineering Materials, A40 (1994).

[15] Castillo, E., Fernández-Canteli, A., A unified statistical methodology for modeling fatigue damage, Springer (2009).

[16] Raposo, P., Correia, J.A.F.O., De Jesus, A.M.P., Calçada, R.A.B., Lesiuk, G., Hebdon, M., Fernández-Canteli, A., Probabilistic fatigue S-N curves derivation for notched components, Frattura ed Integrità Strutturale, 42 (2017) 105-118. DOI: 10.3221/IGF-ESIS.42.12

[17] Correia, J.A.F.O., Huffman, P., De Jesus, A.M.P., Cicero, S., Fernández-Canteli, A., Berto, F., Glinka, G., Unified two-stage fatigue methodology based on a probabilistic damage model applied to structural details, Theoretical and Applied Fracture Mechanics (in press) (2017). DOI: 10.1016/j.tafmec.2017.09.004.

[18] Standard Practice for Statistical Analysis of Linear or Linearized Stress-Life (S-N) and Strain-Life (ε-N) Fatigue Data. ASTM E739 – 10.

[19] Lieurade, H.P., Rupture par fatigue des aciers. Ed. Institut de Recherches de la Sidérurgie Française, collection IRSID-OTUA (1991).

[20] Inglis, N.P., Hysteresis and fatigue of Wöhler rotating cantiveler specimen, The Metallurgist, (1927) 23-27.

[21] Pineau, A., Mécanismes d'accommodation et de fissuration en fatigue oligocyclique, Mécanique Matériaux Electricité, 323/324 (1976) 6-14.

[22] Smith, R.W., Hirschberg, M.H., Manson, S.S., Fatigue behavior of materials under strain cycling in low and intermediate life range, NASA-TN-D-1574, N-63-14250, (1963).

[23] Morrow, J., Cyclic plastic strain energy and fatigue of metals, internal friction, damping and fatigue of metals, ASTM (1965) 48-87.

[24] Gallet, G., Lieurade, H.P., Prévision du comportement en fatigue plastique des aciers de construction mécanique à partir de leurs caractéristiques de traction, Rapport *IRSID* (IRSID, Saint-Germain-en-Laye), (l977).

[25] Halford, G.R., Manson, S.S., Symposium on fatigue, Londres (1967).

[26] Gallet, G., Lieurade, H.P., Influence de la structure métallographique d'un acier au nickel - chrome – molybdène sur son comportement en fatigue plastique, Communication présentée aux Journées Métallurgiques d'Automne organisées par la Société Française de Métallurgie, (1974).

[27] Lemaitre, J., Chaboche, J.L., Mécanique des matériaux solides, Science Sup - 2éme édition, Dunod (2004).

[28] Tomkins, B., Fatigue crack propagation analysis, Philosophical magazine, 155 (1968) 1041-1065.

NOMENCLATURE

A (%)	elongation at fracture
b	fatigue resistance exponent
c	fatigue ductility exponent
E	Young module
K	monotonic hardening coefficient
K'	cyclic hardening coefficient
N	monotonic hardening exponent
n'	cyclic hardening exponent

N_f	number of cycles to failure
UTS	ultimate tensile strength
R	load ration
W_f	total energy to failure
$YS_{0.2\%}$	conventional yield strength at 0.2 of strain
$YS'_{0.2\%}$	conventional yield strength at 0.2 of strain in cyclic tensile
σ_1	stress corresponding to 1% of tensile plastic deformation
σ_a	alternative stress
σ_{amp}	stress amplitude
σ_f	true stress at failure
σ'_f	fatigue resistance coefficient
σ_m	mean stress
σ_{max}	maximum stress
σ_{min}	minimum stress
ε_f	true strain at failure
ε'_f	fatigue ductility coefficient
$\Delta\sigma_1$	Stress variation between the stress levels of the monotonic and cyclic tensile curves for 1% of plastic deformation
$\Delta\varepsilon_{el}$	elastic strain variation
$\Delta\varepsilon_p$	plastic strain variation
$\Delta\varepsilon_t$	total strain variation
ΔW	mechanical strain energy